

Parametric Analysis of Sand Erosion in Pipe Bends Using Computational Fluid Dynamics

Emeka Okafor¹, Ikechukwu Obiuto Ibeneme¹

¹Department of Petroleum and Gas Engineering, University of Port Harcourt, Choba, Port Harcourt, Rivers State, Nigeria

Abstract— Major solid particle erosion may lead to potential failure of upstream oil and gas producing wells. For instance, producing wells with substantial sand production may negatively impact production equipment, well tubing, and pipeline components and fitting, thus leading to costly maintenance routines, production downtime, loss of equipment, and potential environmental damage. This work presents results obtained from investigating parametric factors that determine the extent and severity of sand erosion on pipe bends. We examine the effect of fluid velocity, pipe geometry, pipe degree of bending, bend radius, and sand particle size on erosion severity. The results are based on simulations using an extensively validated proprietary computational fluid dynamic model. It is found that erosion rates increased with both sand particle size (diameter) and fluid velocity, and decreased with bend radius, pipe diameter, and pipe degree of bending. Results also show that it would be possible to determine the threshold magnitudes of the parameters that would result in an assumed threshold erosion rate.

Keywords— Sand erosion, computational fluid dynamics, sand particle, pipe bends.

I. INTRODUCTION

Sand production poses key challenges for oil and gas production, with sand management becoming increasingly important in managing high rate wells. The impingement of sand on fittings and tubing leads to loss of the wall material and when such erosion damage is significant, failure in a relatively short amount of time may result, thereby exposing personnel and equipment to potential safety risks and hazards. It is, therefore, important for upstream oil and gas producers to have the capacity to predict the severity of erosion in these facilities so that the service life of key equipment that can be impacted by erosion can be determined, and then elongated, if practicable. Gaining more insights of the nature and severity of pipe erosion in order to precisely predict the erosion rate and identify the pipe locations which are most susceptible to erosion is of utmost importance and computational Fluid Dynamics (CFD) can be used for predicting pipe erosion rates in different flow conditions and pipe geometries. There has been investigations by Edwards et al. [1] who studied the effects of plugged tees and bend radius on erosion and these workers developed procedures that could be applied within CFD codes for predicting pipe erosion. Their work was experimentally validated for particle penetration rates. Other contributors in this field are noteworthy including Barton [7], Wang and Shirazi [5], McLaury et al. [2], Viera et al. [3], Mansouri et al. [4], Felten [6], Sedrez et al. [14], Lain and Sommerfeld [15], Yusof et al. [16], Wee and Yap [17], and Farokhipour et al. [18].

A. Governing Equations

A number of models exist for modelling liquid-sand flow Abdulla A. [12]. For example, the Eulerian–Lagrangian multiphase flow modelling method which assumes a continuous phase-based solution for the Time-Averaged Navier-Stokes equations can be used to predict erosion rates in pipe bends. Here, the particles are treated as a discrete phase and solved by tracking a large number of individual solid particles, droplets, or bubbles trajectories [12]. For this

approach, the conservation of mass and momentum equations are expressed as,

$$\frac{\partial}{\partial t}(\rho) + \nabla(\rho\vec{v}) = 0 \quad (1)$$

$$\frac{\partial}{\partial t}(\rho\vec{v}) + \nabla(\rho\vec{v}\vec{v}) = -\nabla p + \nabla(\vec{\tau}) + \rho\vec{g} + \vec{S}_m \quad (2)$$

where S_m , is the mass added to continuous phase from dispersed second phase, p is the static pressure, $\vec{\tau}$ is the stress tensor, and $\rho\vec{g}$ is the gravitational body force. The stress tensor equation is given by,

$$\vec{\tau} = \mu \left[(\nabla\vec{v} + \nabla\vec{v}^T) - \frac{2}{3}\nabla\vec{v}I \right] \quad (3)$$

where μ is the molecular viscosity and I is the unit vector tensor. The standard k - ϵ turbulence model originally developed by Launder and Spalding [8] is used to resolve the flow turbulence. The transport equations for the turbulence kinetic energy, k , and the dissipation rate, ϵ , are expressed as,

$$\begin{aligned} \frac{\partial}{\partial t}(\rho k) + \frac{\partial}{\partial x_i}(\rho k u_i) \\ = \frac{\partial}{\partial x_j} \left[\left(\mu + \frac{\mu_t}{\sigma_k} \right) \frac{\partial k}{\partial x_j} \right] + G_k + G_b - \rho\epsilon - Y_M + S_k \end{aligned} \quad (4)$$

$$\begin{aligned} \frac{\partial}{\partial t}(\rho\epsilon) + \frac{\partial}{\partial x_i}(\rho\epsilon u_i) \\ = \frac{\partial}{\partial x_j} \left[\left(\mu + \frac{\mu_t}{\sigma_\epsilon} \right) \frac{\partial \epsilon}{\partial x_j} \right] + C_{1\epsilon} \frac{\epsilon}{k} (G_k + C_{3\epsilon} G_b) \\ - C_{2\epsilon} \rho \frac{\epsilon^2}{k} + S_\epsilon \end{aligned} \quad (5)$$

where G_k is the generation of turbulence kinetic energy due to mean velocity gradients, G_b is the generation of turbulence kinetic energy due to buoyancy, Y_M is the contribution of fluctuating dilation in compressible turbulence to the overall dissipation rate, σ_k is the turbulent Prandtl number for k , σ_ϵ is the turbulent Prandtl number for ϵ , S_k is the user-defined source term, S_ϵ is the user-defined source term, and $C_{1\epsilon}$, $C_{2\epsilon}$, and $C_{3\epsilon}$ are constants. The trajectory of each particle is predicted by solving the particle force balance, as expressed in Equation 7,

$$\mu_t = \rho C_\mu \frac{k^2}{\epsilon} \quad (6)$$

$$\frac{d\mathbf{u}_p}{dt} = F_D(\vec{\mathbf{u}} - \vec{\mathbf{u}}_p) + \frac{\vec{g}(\rho_p - \rho)}{\rho_p} + \vec{F} \quad (7)$$

where \vec{F} is the acceleration term, $F_D(\vec{\mathbf{u}} - \vec{\mathbf{u}}_p)$ is the drag force per unit particle mass. The drag force is computed using the following relationship,

$$F_D = \frac{18\mu C_D Re}{\rho_p d_p^2 24} \quad (8)$$

where \mathbf{u} is carrier fluid velocity, \mathbf{u}_p is the particle velocity, μ is molecular viscosity of fluid, ρ is the fluid density, ρ_p is the particle density, d_p is the particle diameter, C_D is the drag coefficient, and Re is the Relative Reynolds Number. The relative Reynolds Number, Re , is calculated from the following relationship,

$$Re = \frac{\rho d_p |\vec{\mathbf{u}} - \vec{\mathbf{u}}_p|}{\mu} \quad (9)$$

The drag coefficient, C_D is computed based on spherical drag law, in which the C_D is given by Equation (10),

$$C_D = a_1 + \frac{a_2}{Re} + \frac{a_3}{Re^2} \quad (10)$$

where, a_1 , a_2 and a_3 are constants that apply over a wide range of Re given by Morsi and Alexander [9]. Finally, after calculating the flow of liquid and the discrete phase through the model, the proprietary simulator can calculate the rate of erosion [12] given by,

$$R_{erosion} = \sum_{p=1}^{N_{Particles}} \frac{\dot{m}_p C(d_p) f(\alpha) v^{b(v)}}{A_{face}} \quad (11)$$

where \dot{m}_p is the particle mass flow rate, $C(d_p)$ is the function of particle diameter, α is the impact angle of particle path with wall face, $f(\alpha)$ is the function of impact angle, v is the relative particle velocity, $b(v)$ is the function of relative particle velocity, and A_{face} is the area of cell face. C , f and b are constant functions, and the numerical values of these functions depend on the properties of pipe material. The values specified for the functions C , f and b are 1.8×10^{-9} , 1 and 0, respectively, as recommended by Mazumder [10].

The CFD approach described above is very advantageous when modelling particle flow interaction, collision, and wall interaction but at high computational cost, most especially, when two way coupling is considered between continuous flow and particles.

B. Pipe Bends

It is necessary to have a thorough understanding of the nature and severity of erosion in order to precisely predict the erosion rate and identify pipe locations most susceptible to erosion (see Figure 1). It has been well-understood that pipe bends are most susceptible to damage caused by sand as such components alter the direction in which the production fluid is flowing. The erosion phenomenon is highly complicated due to the number of parameters affecting the erosion severity, such as production flow rate, sand rate, fluid properties, flow regime, sand properties, sand shape and size, wall material of equipment, and geometry of the equipment.

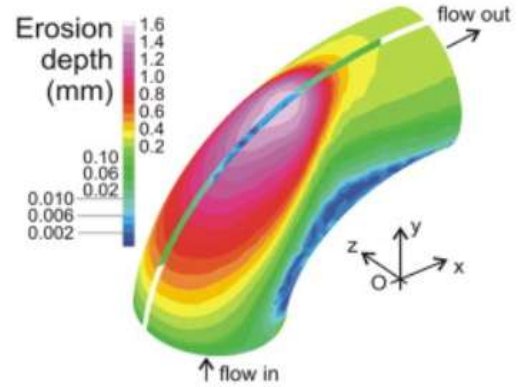


Figure 1: Section of Erosion in a Standard Pipe Elbow [11].

C. Computational Fluid Dynamics (CFD)

Computational Fluid Dynamics (CFD) is a part of fluid mechanics that applies numerical methods and algorithms for the solution and analysis of problems that relates to fluid flows. Here, we use a proprietary CFD model to build a 'virtual prototype' of our system and then apply real-world physics and chemistry to the model, and this is immediately followed up with post-processing and performance prediction of the CFD model for pipe bends.

II. METHODOLOGY

D. Solution Steps

This investigation is carried out using a proprietary CFD simulator [13] which solves erosion and transport equations of mass, momentum, energy conservation, and species concentration. The organizational program structure of this simulator involves a CAD design linked to three key actions, namely: meshing, grid compilation and computations by solver. The meshing activity includes the setting of geometry along with a 2D or 3D mesh. The solver activities include mesh importation and adaptation, physical models, boundary conditions, material properties, calculation, and post-processing. The grid compilation may include a 2D triangular mesh, a 3D tetrahedral mesh and a 2D/3D hybrid mesh. The proprietary simulator discretizes the partial differential equations and takes the following general steps in modeling both fluid flow and heat transfer: (1) The pre-processing phase uses the Design-Modeler in geometry definition, meshing, and boundary conditioning; (2) The processing phase solves relevant equations by identifying appropriate choices for solution parameters; and (3) The post-processing phase analyzes all results obtained from CFD simulations.

E. Model Development

Figure 2 shows the results of a processing activity – a 3-D geometry of the bend pipe while Fig. 3 shows the hexahedral mesh structure of the bend pipe geometry. The meshing is carefully done as to accurately resolve the flow in the pipe near wall. We use both surface and volume meshing and ran mesh diagnostics to assure mesh quality. The rate of erosion is computed using equation 11.



Figure 2: Geometry of the Pipe Model with the Named Sections

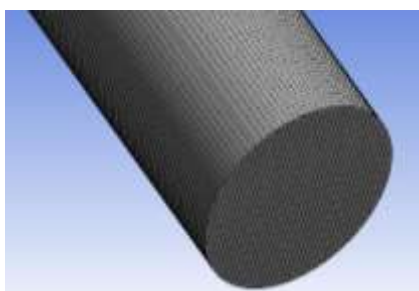


Figure 3: Computational Mesh Used In the Simulation [13]

III. RESULTS AND DISCUSSION

The effect of five parameters including flow velocity, pipe diameter, sand particle size, bend radius and degree of pipe bending will be discussed in this section.

F. Model Parameters

This parametric study illustrates the analysis of the simulation of erosion rate in pipeline bends and the sensitivity of erosion rate to variation in the magnitude of the parameters already indicated above. Table 1 shows a summary of the specific parameters used in this work.

Table 1: Properties for Setting up The Model in the proprietary simulator

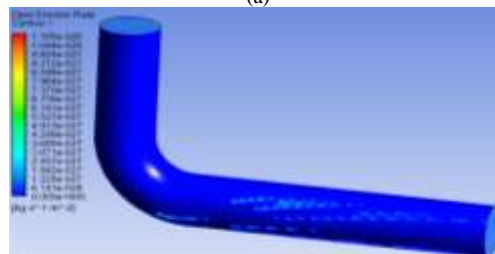
Time	Steady
Temperature	30 °C
Continuous phase	Methane gas
Pipe diameters	4 inches, 6 inches, 12 inches
Pipe radius curvature	4 inches, 7 inches, 12 inches
Pipe bending degrees	45°, 90°, 120°
Dispersed phase	Sand particles
Inlet fluid velocity	0.65 m/s, 3 m/s, 5 m/s
Sand particle diameter	1e-06 m, 1e-05 m, 1e-07 m
Total flow rate	1e-20 kg/s
Sand particle material	Spherical shaped Anthracite
Particle density	1550 kg/m ³
Particle type	Inert
Turbulence model	K -Epsilon (k-ε) turbulence model
K-Epsilon Turbulence	Realizable Two-Layer K-Epsilon
Gravita. acceleration	9.81 m/s ²
Max. no of steps	2500
Iteration	300
Mesh	Cutcell, Inflation and Body sizing
Mesh element size	0.005

G. Effect of Pipe Diameter

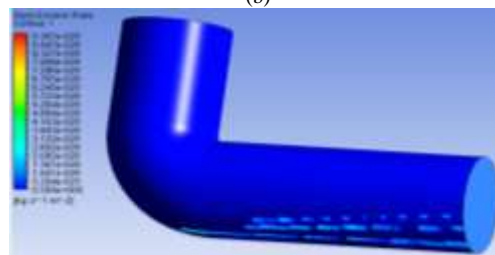
Figure 4a, 4b, and 4c show the effect of pipe diameter on erosion rate for 4-inch, 6-inch and 12-inch pipe diameter test geometries, respectively. Figure 4d shows the computed maximum erosion rate versus pipe diameter. As can be seen, the surface area increases as the pipe diameter is increased whereas the maximum erosion is reduced. A relatively larger pipe diameter results in a smaller maximum erosion rate and it can be observed also that this reduction is by about 17%, and further by about 92%, when pipe diameter doubled to 12 inches. We can deduce an economic advantage from these results since the service life of pipe bends can be elongated, thereby reducing expenditure on maintenance and repair. However, we need to factor in the fact that higher expenditure, and even platform space allocation issues, may arise with larger piping diameter. So it is important to consider the feasibility of redesigning relatively larger pipes as an erosion mitigating measure while ensuring overall lower expenditure.



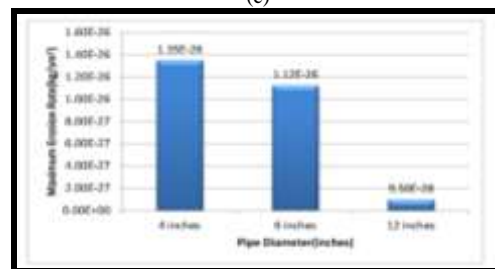
(a)



(b)



(c)



(d)

Figure 4: (a) Erosion Profile of Pipe Bend with 4-inch Pipe Diameter; (b) Erosion Profile of Pipe Bend with 6-inch Pipe Diameter; (c) Erosion Profile of Pipe Bend with 12-inch Pipe Diameter (d) Maximum Erosion Rate versus Pipe Diameter.

H. Effect of Pipe Degree of Bending

Figure 5a, 5b, and 5c show the effect of pipe degree of bending on erosion rate for 45°, 90°, and 120° test geometries, respectively. A drop in maximum erosion rate is observed with an increasing pipe degree of bending. This suggests that the site of erosion damage is also decreased. Figure 5d shows the recorded maximum erosion rate values for each bending degree. Increasing the bending degree from 45° to 90° decreased the maximum erosion by 17%. Further decrease from 90° to 120° reduces the maximum erosion rate by 82%. Therefore, caution should be exercised when designing pipelines with the objective to increase the life span and durability of the pipes. Where possible, an optimum bending degree during design should always be targeted.

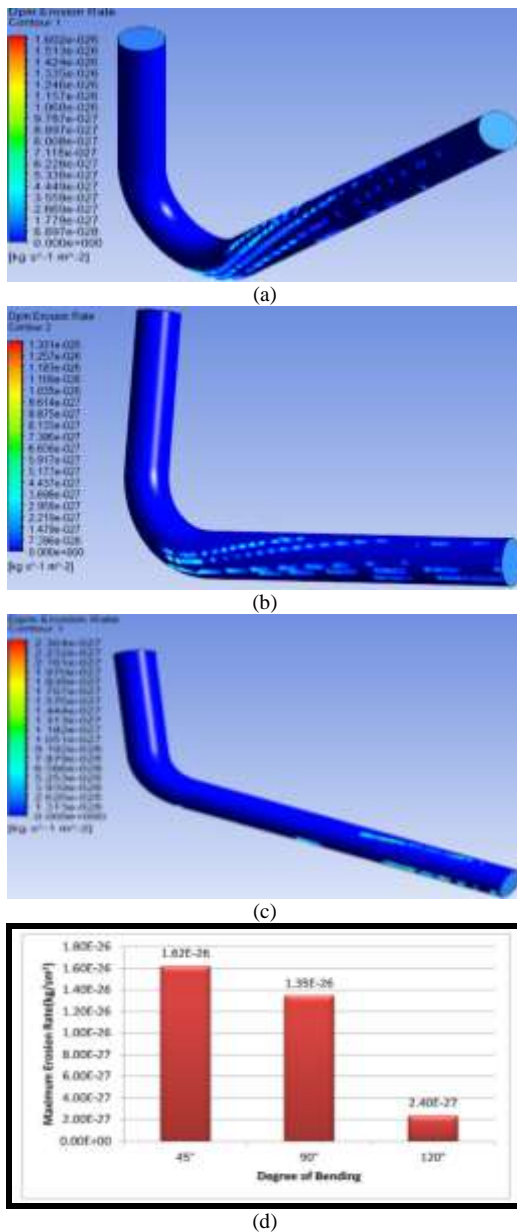


Figure 5: (a) Erosion Profile of Pipe with Bending Degree 45°; (b) Erosion Profile of Pipe with Bending Degree 90°; (c) Erosion Profile of Pipe with Bending Degree 120°; (d) Maximum Erosion Rate versus Pipe Bending Degree

I. Effect of Bend Radius

Figure 6a, 6b, and 6c show the effect of bend radius on erosion rate for 4-inch, 7-inch and 12-inch bend radius test cases, respectively, and it is evident from these figures that altering the pipe bend radius has a significant effect on the magnitude and overall shape of the erosion. Figure 6d shows that the maximum erosion rate reduces with increasing bend radius and this is in agreement with the results of Wang and Shirazi [5], who found that maximum erosion rate, decreases with increasing bend radius for gas-solid flows. When bend radius increased from 4 inches to 7 inches, the maximum erosion reduced by 32%. And further increasing the bend radius from 7 inches to 12 inches resulted in a 20% reduction in erosion. The advantages of increasing the bend radius is, again, obvious in terms of life span and cost of maintenance and repair. Though the weight of piping may triple as a result. However, a proper economic evaluation of the design expenditure will minimize the economic and platform space disadvantages.

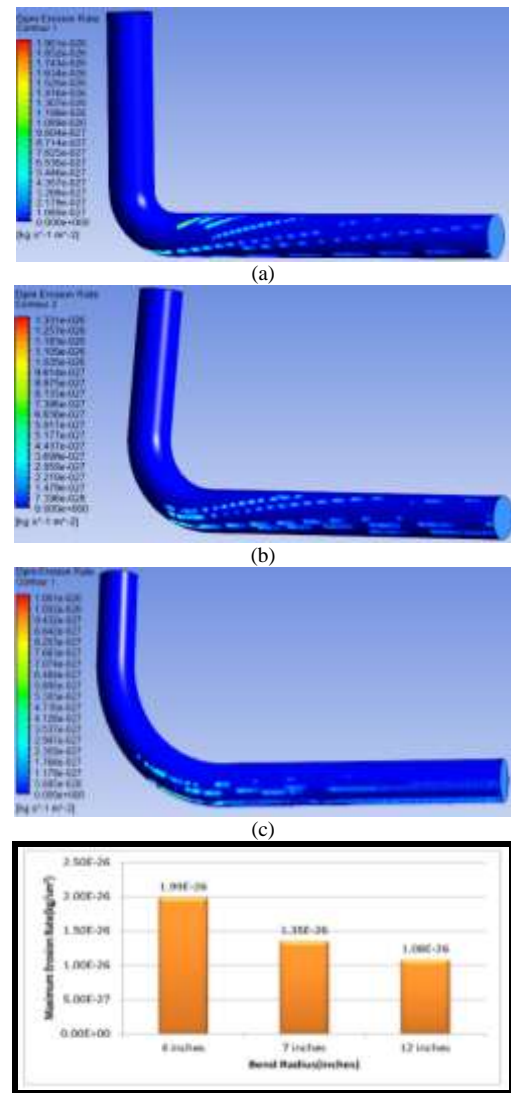


Figure 6: (a) Erosion Profile of Pipe Bend with 4-inch Bend Radius; (b) Erosion Profile of Pipe Bend with 7-inch Bend Radius; (c) Erosion Profile of Pipe Bend with 12-inch Bend Radius; (d) Maximum Erosion Rate versus Bend Radius

Pipe Bend with 12-inch Bend Radius; (d) Maximum Erosion Rate versus Bend Radius

J. Effect of Fluid Velocity

Figure 7a, 7b, and 7c show the erosion profiles for different inlet fluid velocity. It shows clearly that increasing the fluid velocity increases the erosion rate in the pipes. Figure 7d shows the recorded maximum erosion rate values for each fluid velocity. Increasing the fluid velocity from 0.65m/s to 3m/s is seen to increase the maximum erosion occurring by around 88%. Thus, while designing pipelines, the fluid velocities within the pipes should be considered.

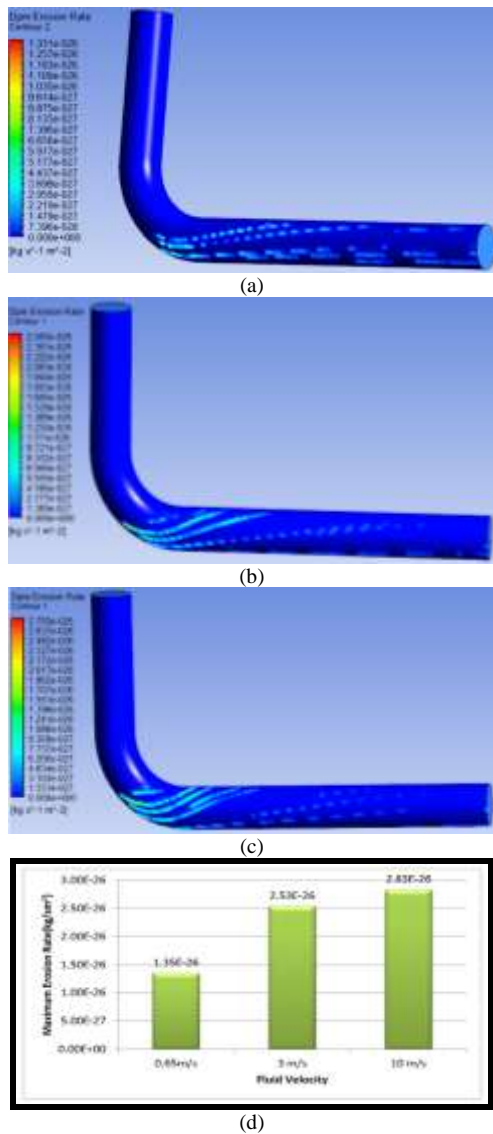


Figure 7: (a) Erosion Profile of Pipe Bend with Fluid Velocity of 0.65m/s; (b) Erosion Profile of Pipe Bend with Fluid Velocity of 3m/s; (c) Erosion Profile of Pipe Bend with Fluid Velocity of 10 m/s; (d) Maximum Erosion Rate versus Fluid Velocity.

K. Effect of Particle Size

Figure 8a, 8b, 8c and 8d show the effect of the sand particle size on erosion rate for 1e-07m, 1e-06m, 1e-08m sand particle diameter, respectively. Maximum erosion rate and area affected by erosion increases as the sand particle diameter

increases. Increasing the sand particle diameter, from 1e-07m to 1e-06m, increases the maximum erosion by 6% and further increasing the sand particle diameter from 1e-06m to 1e-05m resulted in 81% increase in the maximum erosion. Thus, the physical properties of sand should be factored in when designing pipe for erosion management.

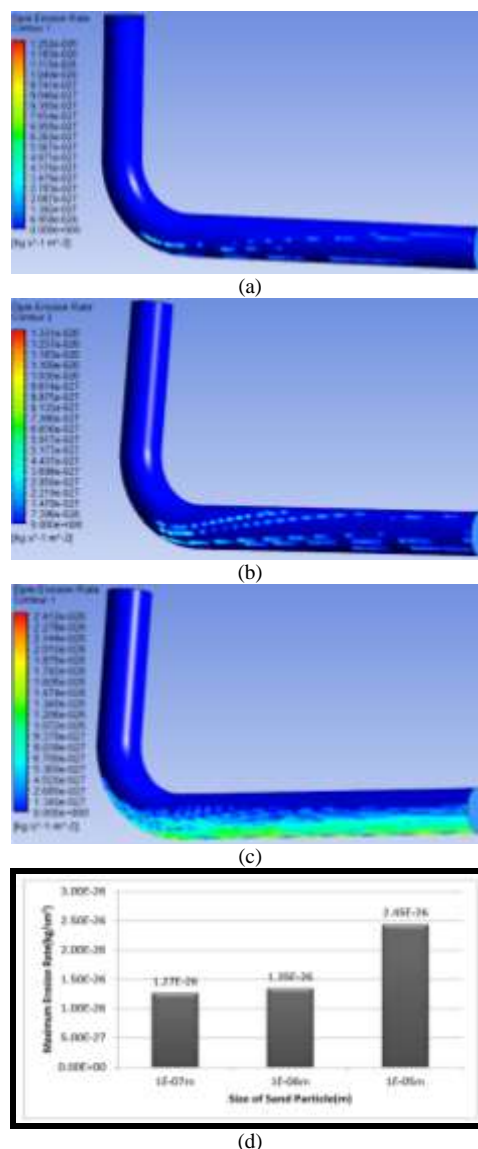


Figure 8: (a) Erosion Profile of Pipe Bend with Sand Particle Diameter 1e-07m; (b) Erosion Profile of Pipe Bend with Sand Particle Diameter 1e-06m; (c) Erosion Profile of Pipe Bend with Sand Particle Diameter 1e-05m; (d) Maximum Erosion Rate versus Size of Sand Particle

IV. CONCLUSION

In this work, a proprietary CFD based simulation model is used to study the effects of some parametric factors on erosion rate in pipe bends. The effect of five parameters were studied, namely, pipe diameter, pipe degree of bending, fluid velocity, sand particle size and bend radius. Erosion rate was found to increase with carrier fluid velocity and sand particle diameter but decreased with increasing bend radius, fluid velocity, and pipe degree of bending. The results provide clear indications of how varying such parameters can influence the magnitude

of erosion and how often repair and replacement work is required. The results also provide insight on how best to redesign a pipeline to minimize the negative impact of erosion, most especially, at pipe bends.

REFERENCES

- [1] Edwards, J., McLaury B., Shirazi, S., "Modeling Solid Particle Erosion in Elbows and Plugged Tees," *Journal of Energy Resources Technology*, vol. 123, issue 4, pages 277-284, 2001.
- [2] McLaury, B., Shirazi, S., Viswanathan, V., Mazumder, Q., Santos, G., "Distribution of Sand Particles in Horizontal and Vertical Annular Multiphase Flow in Pipes and the Effects on Sand Erosion," *Journal of Energy Resources Technology*, vol. 133, issue 2, pages 1 -10, 2011.
- [3] Viera, R., Kesena, N., McLaury, B., Shirazi, S., "Sand Erosion in Multiphase Flow for Low-Liquid Loading and Annular Conditions.," *ASME 2012 International Mechanical Engineering Congress and Exposition*, Texas, vol.7, issue 1, 2012.
- [4] Mansouri, A., Shirazi, S., McLaury, B., "Experimental and Numerical Investigation of the Effect of Viscosity and Particle Size on the Erosion Damage Caused by Solid Particles," *ASME 2014 4th Joint US-European Fluids Engineering Division Summer Meeting collocated with the ASME 2014 12th International Conference on Nanochannels, Microchannels, and Minichannels*, Chicago, 2014.
- [5] Wang, J., Shirazi, S., "A CFD Based Correlation for Erosion Factor for Long-Radius Elbows and Bends," *Journal of Energy Resources Technology*, vol. 125, issue 1, pages 26-34, 2003.
- [6] Felten, F., "Numerical Prediction of Solid Particle Erosion for Elbows Mounted in Series," *ASME 2014 4th Joint US-European Fluids Engineering Division Summer Meeting collocated with the ASME 2014 12th International Conference on Nanochannels, Microchannels, and Minichannels*, Chicag, pages 23-33, 2014.
- [7] Barton, N., "Erosion in Elbows in Hydrocarbon Production Systems: Review Document," HSE Books, Colgate, Norwich, Rep. 115, 2003.
- [8] Launder, B. E., and Spalding, D. B., "The numerical computation of turbulent flows," *Computer Methods In Applied Mechanics And Engineering*, vol. 3, issue 2, pages 269-289, 1974.
- [9] Morsi, S., Alexander, A. J., "An investigation of particle trajectories in two-phase flow systems," *Journal of Fluid Mechanics*, vol. 55, issue 02, pages 193-208, 1972.
- [10] Mazumder, Q., "Tutorial: Investigate Erosion In A 180 Degree U-Bend Using FLUENT", Computational Fluid Dynamics Research Center, 2019. Available: site/path/file: <https://www.coursehero.com/file/15178402/TUTORIAL-INVESTIGATE-EROSION-IN-A-180-DEGREE-U-BEND-USING-FLUENT/>.
- [11] Solnordal, Christopher B., Wong, Chong Y., Boulanger, Joan, "An experimental and numerical analysis of erosion caused by sand pneumatically conveyed through a standard pipe elbow," *Wear*, vol. 336-337,, pages 43-57, 2015.
- [12] A. Abdulla, "Estimating erosion in oil and gas pipeline due to sand presence," M.S. Thesis, Department of Mechanical Engineering, Blekinge Institute of Technology, Karlskrona., Sweden, 2011.
- [13] ANSYS Fluent (2009), 12.0/12.1 Documentation, Users Guide Manual, Ansys Inc., 2009.
- [14] Sedrez., T. A., Shirazi, S. A., Rajkumer, W., Sambath, K., Subramani, H. J., "Experiments and CFD simulations of erosion of a 90° elbow in liquid-dominated liquid-solid and dispersed-bubble-solid flows," *Wear*, vol. 424-427, pages 570-580, 2019.
- [15] Lafn, S., and Sommerfeld, M. "Numerical prediction of particle erosion of pipe bends," *Advanced Powder Technology*, vol. 30, issue 2, pages 366-383, 2019.
- [16] Yusof, M. A. H., Zakaria, Z., Supee, A., Yusop, M. Z. M. and Haladin, N. B., "Prediction of Erosion Rate in Elbows for Liquid-Solid Flow via Computational Fluid Dynamics (CFD)," *Applications Of Modelling And Simulation*, vol. 3, issue 1, pages 28-38, 2019.
- [17] Wee, S. K., and Yap, Y.J., "CFD study of sand erosion in pipeline," *Journal of Petroleum Science and Engineering*, vol. 176, pages 269-278, 2019.
- [18] Farokhipour, A., Mansoori, Z., Rasteh, A., Rasoulia, M. A., SaffarAvval, M., and Ahmadi, G., "Study of erosion prediction of turbulent gas-solid flow in plugged tees via CFD-DEM," *Powder Technology*, vol. 352, pages 136-150, 2019.